

# Manifestation of finite temperature size effects in nanogranular magnetic graphite

S. Sergeenkov<sup>1</sup>, N.S. Souza<sup>1</sup>, C. Speglich<sup>1</sup>, V.A.G. Rivera<sup>1</sup>, C.A.

Cardoso<sup>1</sup>, H. Pardo<sup>2</sup>, A.W. Mombrou<sup>2</sup> and F.M. Araújo-Moreira<sup>1</sup>

<sup>1</sup>Materials and Devices Group, Department of Physics and Physical Engineering,  
Universidade Federal de São Carlos, São Carlos, SP, 13565-905 Brazil

<sup>2</sup>Crystallography, Solid State and Materials Laboratory (Crysmat-Lab),

DEQUFIM, Facultad de Química, Universidad de la República,

P.O. Box 1157, CP 11800, Montevideo, Uruguay

(Dated: April 2, 2024)

In addition to the double phase transition (with the Curie temperatures  $T_C = 300\text{K}$  and  $T_{C_t} = 144\text{K}$ ), a low-temperature anomaly in the dependence of the magnetization is observed in the bulk magnetic graphite (with an average granular size of  $L \approx 10\text{nm}$ ), which is attributed to manifestation of the size effects below the quantum temperature  $T_L / k_B = L^2$  and is well fitted by the periodic function  $M_L(T) / \sin[M(T)]$  ( $T=L$ ) with  $M(T)$  being the bulk magnetization and  $(T) / k_B = T$  the thermal de Broglie wavelength. The best fits of the high-temperature data (using the mean-field Curie-Weiss and Bloch expressions) produced reasonable estimates for the model parameters, such as defects mediated effective spin exchange energy  $J \approx 12\text{meV}$  (which defines the intragranular Curie temperature  $T_C$ ) and proximity mediated interactions between neighboring grains (through potential barriers  $U$  created by thin layers of non-magnetic graphite) with energy  $J_t = \exp(-d/\lambda) J \approx 5.8\text{meV}$  (which defines the intergranular Curie temperature  $T_{C_t}$ ) with  $d \approx 1.5\text{nm}$  and  $\lambda/k_B \approx 2\text{nm}$  being the intergranular distance and characteristic length, respectively.

PACS numbers: 75.50.Dd, 78.70.2g, 81.05.Jw

Recent advances in developing nanographitic systems re-kindled interest in their nontrivial magnetic and transport properties important for numerous applications (for recent reviews, see, e.g., [1, 2, 3] and further references therein). Special attention has been paid to the properties mediated by various defect structures (including pores, edges of the planes, chemically induced vacancies, dislocations, tracks produced by particle irradiation, etc) believed to be responsible for room-temperature ferromagnetism based on (super) exchange between localized spins at defect sites. The existence of sufficiently robust ferromagnetic (FM) like magnetization loops has been successfully proved in highly-oriented pyrolytic graphite (HOPG) [4], proton-irradiated graphite [5], nanographite [6], graphite containing topographic defects [7], negative curvature Schwarzite-like carbon nanofoams [8], fullerene-related carbons [9], microporous carbon [10], and carbon nanohorns [11]. Recently, some interesting results have been reported [12] regarding unusual magnetic properties of Ag nanoparticles encapsulated in carbon nanospheres (with  $\approx 10\text{nm}$  diameter) interconnected in necklace-like structures which have a tremendous potential for applications in electronics, biotechnology and medicine.

In this paper, we report our latest results on the temperature dependence of the magnetization in bulk room-temperature magnetic graphite (MG) with an average grain size of  $L \approx 10\text{nm}$ . Several interesting features have been observed in our MG samples, including (i) the double transition with the Curie temperatures  $T_C = 300\text{K}$  and  $T_{C_t} = 144\text{K}$  attributed, respectively, to the manifestation of the intragranular  $M_p(T)$  and in-

tergranular  $M_t(T)$  contributions to bulk magnetization  $M(T)$ , and (ii) a low-temperature anomaly in the dependence of  $M(T)$ , attributed to manifestation of the finite temperature size effects below the quantum temperature  $T_L / k_B = L^2$ .

Our MG samples were produced by a vapor phase redox controlled reaction in closed nitrogen atmosphere with addition of copper oxide using synthetic graphite powder (more details regarding the patented chemical route for synthesis of the discussed here magnetic graphite can be found elsewhere [13, 14]). To avoid presence of any kind of FM impurity, we have carefully determined the chemical purity of the samples with atomic absorption spectroscopy (AAS) using a Shimadzu AA 6800 spectrometer and checked these results with X-ray fluorescence analysis (XRF) and energy dispersive spectroscopy (EDS), comparing the results obtained for the pristine (non-magnetic) and the modified (magnetic) graphite. The structure of MG samples has been verified by Raman spectroscopy, X-ray diffraction (XRD) and scanning electron microscopy (SEM). These studies were performed using Seifert Scintag PAD-II powder diffractometer, with  $\text{CuK}$  radiation ( $\lambda = 1.5418\text{\AA}$ ) and Jeol JSM 5900LV microscope, respectively. In addition to the broader (as compared with the pristine non-magnetic graphite) peak at  $1580\text{cm}^{-1}$ , corresponding to chemically modified magnetic graphite, our micro Raman analysis shows the appearance of a new peak at  $1350\text{cm}^{-1}$  (known as the disordered D band) in the MG sample. In turn, the XRD profiles revealed that the peaks of the magnetic graphite for (002) and (004) reflections are wider and asymmetric, with a visible compression of c-axis (due to

chemically induced defects in the MG structure) that facilitates bringing the graphene layers closer to each other (thus further enhancing FM properties of the sample). To verify the correlation between the microstructural features (topography) and the presence of magnetic regions in MG sample, we also used the atomic force (AFM) and magnetic force (MFM) microscopy. The comparison of the obtained AFM and MFM 3D images (along with the corresponding SEM images) revealed that our MG sample is a rather dense agglomeration of spherical particles (with diameters of  $L \approx 10\text{nm}$ ) coated by thin layers of non-reacted pristine (non-magnetic) graphite (with thickness of  $d \approx 1-2\text{nm}$ ), producing both intra- and intergranular magnetic response.

The magnetization measurements were done using a MPMS-5T Quantum Design magnetometer. Both zero-field cooled (ZFC) and field-cooled (FC)  $M-T$  cycles were measured. From the  $M-H$  hysteresis loop for MG sample (with mass  $0.4\text{mg}$ ) taken at  $T = 295\text{K}$  and after subtracting diamagnetic background (equivalent to  $1.2 \cdot 10^{-3} \text{B}$  per carbon atom), we deduced  $M_s = 0.25 \text{emu/g}$ ,  $M_r = 0.04 \text{emu/g}$  and  $H_c = 3500 \text{e}$  for the room-temperature values of saturation magnetization, remnant magnetization and coercive field, respectively. The temperature behavior of the normalized ZFC magnetization  $M(T)/M(T_p)$  in our MG sample (taken at  $H = 1\text{kOe}$ ) is shown in Fig.1 after subtracting the diamagnetic and paramagnetic contributions ( $T_p = 0.16T_C = 48\text{K}$  is the temperature where  $M(T)$  has a maximum with the absolute value of  $M(T_p) = 0.12 \text{emu/g}$ ). First of all, notice that there are two distinctive regions, below and above the peak temperature  $T_p$ . Namely, below  $T_p$  there is a well-defined low-temperature minimum (around  $T_m = 0.05T_C = 15\text{K}$ ), while for  $T > T_p$  we have a crossover region (near  $T_0 = 0.38T_C = 114\text{K}$ ) indicating the presence of a double phase transition in our sample. More precisely, in addition to the phase with the Curie temperature  $T_C = 300\text{K}$ , there is a second transition with  $T_{Ct} = 0.48T_C = 144\text{K}$ .

Let us begin our discussion with the high-temperature region (above  $T_p$ ). By attributing  $T_C$  and  $T_{Ct}$  to the manifestation of the intrinsic  $M_p$  and extrinsic (intergranular)  $M_t$  contributions to the observed magnetization  $M(T)$ , respectively, we were able to successfully fit our data using the following expressions:

$$M(T) = M_p(T) + M_t(T) \quad (1)$$

with

$$M_p(T) = M_{sp} \tanh \left[ \frac{T_C}{T} \right] \quad (2)$$

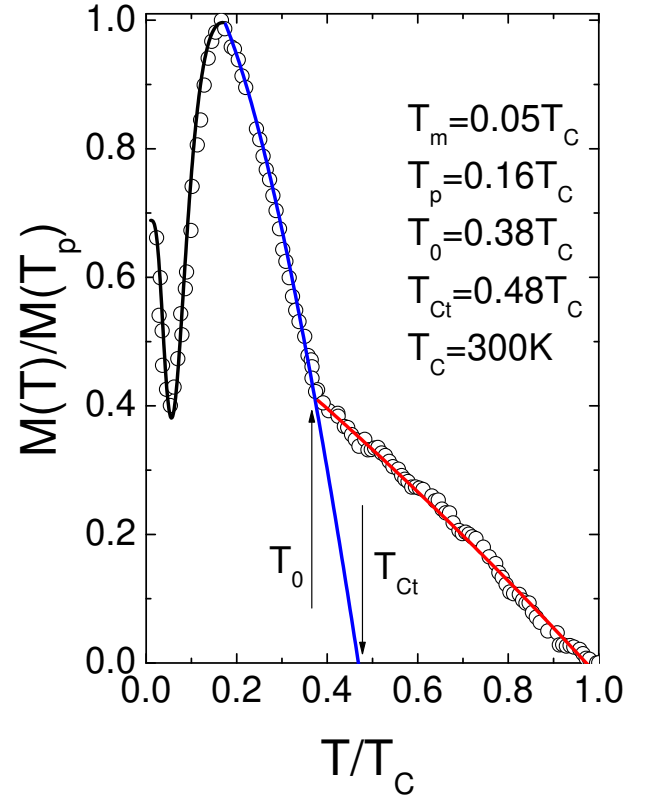


FIG. 1: The temperature dependence of the normalized magnetization  $M(T)$  of magnetic graphite. The solid lines are the best fits according to Eqs.(1)–(4).

and

$$M_t(T) = M_{st} \tanh \left[ \frac{T_{Ct}}{T} \right] \quad (3)$$

The first terms in the rhs of Eqs.(2) and (3) present analytical (approximate) solution of the Curie-Weiss mean-field equation for spontaneous magnetization valid for all temperatures (see, e.g., [15, 16]), while the second terms account for the Bloch (magnon) contributions [17]. The solid lines in Fig.1 present the best fits for high-temperature region ( $T > T_p$ ) according to Eqs.(1)–(3) with the following set of parameters (in terms of the experimental value of the total magnetization  $M(T_p) = 0.12 \text{emu/g}$ ):  $M_{sp} = 0.59M(T_p)$ ,  $M_{mp} = 0.11M(T_p)$ ,  $T_C = 300\text{K}$ ,  $M_{st} = 0.29M(T_p)$ ,  $M_{mt} = 0.05M(T_p)$ , and  $T_{Ct} = 144\text{K}$ . Notice that the above estimates suggest quite a significant contribution from the intergranular interactions ( $M_t \approx 0.5M_p$ ).

To better understand the origin of the model parameters, recall that, according to recent theoretical analysis [5, 12, 18], the room-temperature FM in graphite is most likely due to superexchange mediated by the two different sites in the graphite lattice leading to a FM

coupling between localized spins  $S$  at the defect sites with an effective exchange energy  $J$ , related to the intragranular Curie temperature  $T_C = S(S+1)zJ/3k_B$  (here  $z$  is the number of nearest neighbors). As is well-known, graphite is made of two-dimensional layers in which each carbon is covalently bonded to three other carbons. Atoms in other layers are much further away and are not nearest neighbors, so the coordination number of a carbon atom in graphite is  $z = 3$ . Using  $S = 1/2$  and the experimentally found  $T_C = 300\text{K}$ , we obtain  $J \approx 12\text{meV}$  for a reasonable estimate [5, 18] of the defects mediated spin exchange coupling energy (responsible for the intragranular contribution  $M_p(T)$ ). Besides, within this scenario, the deduced from our M-H hysteresis loops value of the room-temperature saturation magnetization  $M_s = 0.25\text{emu/g}$  corresponds to defect concentration of  $\sim 600\text{ppm}$ , which is within the range reported for nanographite-based carbon materials [19] and is high enough to account for the observed strong FM-like response.

At the same time, given the above-discussed chemically modified nanogranular structure in our sample, it is quite reasonable to assume that the second transition with  $T_{Ct} = 144\text{K}$  (responsible for the intergranular contribution  $M_t(T)$ ) is related to the proximity mediated tunneling of the delocalized spins between neighboring grains (through potential barriers  $U$  created by thin layers of pristine non-magnetic graphite) with the probability  $J_t = \exp(-d/\lambda)$ . Here,  $d$  is the distance between adjacent particles and  $\lambda = \hbar^2/2mU$  is a characteristic length with  $m$  being the effective mass. According to this scenario, the intergranular Curie temperature  $T_{Ct}$  is related to its intragranular counterpart as  $T_{Ct} = \exp(-d/\lambda)T_C$ . Furthermore, by correlating the crossover temperature  $T_0 = 0.38T_C$  with the value of the intergranular barrier  $U \approx k_B T_0$ , we obtain  $U \approx 8\text{meV}$  for its estimate (assuming free electron mass for  $m$ ) which, in turn, brings about  $\lambda \approx 2\text{nm}$  for an estimate of the characteristic length. Moreover, using the found values of the Curie temperatures ( $T_C = 300\text{K}$  and  $T_{Ct} = 144\text{K}$ ), we obtain  $d \approx 1.5\text{nm}$  as a reasonable estimate for an average thickness of non-magnetic graphite layer between magnetic particles in our MG sample. It is also interesting to observe that, given the above obtained value for the tunneling exponent  $\exp(-d/\lambda) \approx 0.48$ , the relations between the intra- and intergranular fitting parameters,  $M_{st} = 0.49M_{sp}$  and  $M_{mt} = 0.47M_{ms}$ , are in good agreement with the proximity mediated scenario, assuming  $M_{st} = \exp(-d/\lambda)M_{sp}$  and  $M_{mt} = \exp(-d/\lambda)M_{ms}$  for the Curie-Weiss and Bloch magnetizations.

Let us turn now to the low-temperature region ( $T < T_p$ ) and discuss the origin of the observed minimum of magnetization near  $T_m = 0.05T_C$ . We will show that this anomaly can be attributed to the quantum size effect. Recall that the finite temperature quantum effects manifest themselves for the size of the system  $L < \lambda(T)$

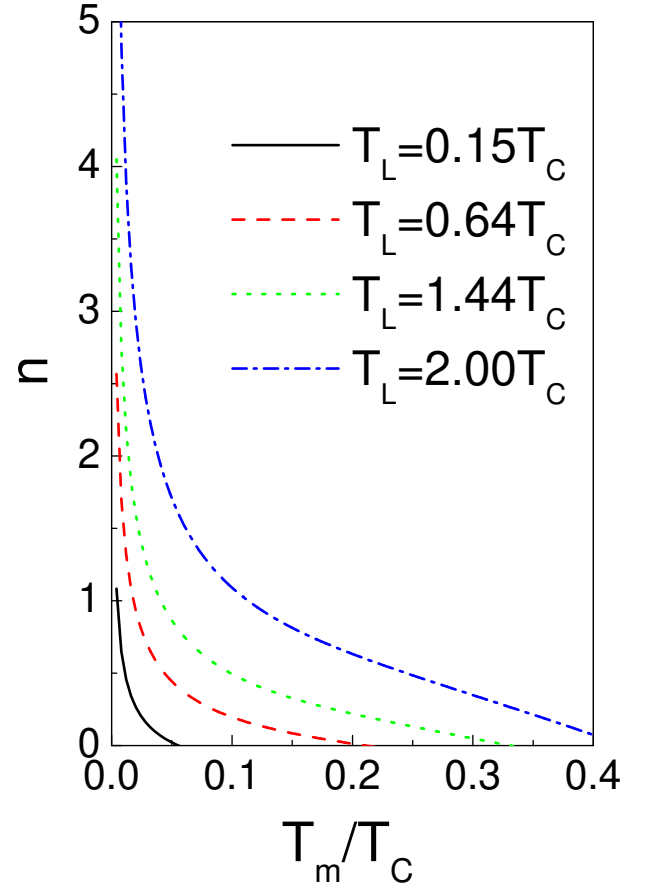


FIG. 2: The dependence of the oscillations  $\Delta$  in  $\Delta$  on reduced temperature  $T_m = T_C$  for different values of the particle size  $L$  related quantum temperature  $T_L$ , according to Eqs.(1)-(4).

where  $\lambda(T) = \frac{2\pi\hbar^2}{m k_B T}$  is the thermal de Broglie wavelength) or, alternatively, for temperatures  $T < T_L$  (where  $T_L = \frac{2\pi\hbar^2}{m k_B L^2}$  is the quantum temperature). Using  $L \approx 10\text{nm}$  for an average size of the single particle in our samples (and assuming free electron mass for  $m$ ), we get  $T_L = 0.15T_C = 45\text{K}$  for the onset temperature below which the manifestation of quantum size effects is expected (notice that  $T_L$  is very close to the peak temperature  $T_p = 0.16T_C$ ). To fit the low-temperature experimental data, we assume the following normalized (to the peak temperature  $T_p$ ) periodic dependence of the finite-size magnetization:

$$\frac{M_L(T)}{M_L(T_p)} = \frac{L}{\lambda(T)} \sin \frac{M(T)}{M(T_p)} \frac{\lambda(T)}{L} \quad (4)$$

where  $M(T)$  is the above-considered total bulk magnetization (thus we assume that quantum effects will influence both intra- and intergrain properties). It can be easily verified that Eq.(4) reduces to  $M(T)$  when the quantum effects become negligible. More precisely,

$M(T) = M(T_p) = \lim_{L \rightarrow \infty} [M_L(T) - M_L(T_p)]$ . The behavior of the low-temperature region ( $T < T_p$ ) using Eqs.(1)–(4) is shown by thick solid line in Fig.1. Notice also that, for a given temperature, the above periodic function  $M_L(T)$  has a minimum at  $T = T_m$  where  $T_m$  is the solution of the following equation,  $M(T_m) = (n+1)M(T_p)L$  with  $n = 0; 1; 2; \dots$  being the number of the oscillation minima. Using the explicit temperature dependencies of the total bulk magnetization  $M(T)$  (given by Eqs.(1)–(3)) and the previously defined thermal de Broglie wavelength  $\lambda(T)$ , in Fig.2 we depict the solution of the above equation as the dependence of the quantization minima on reduced temperature  $T_m = T_c$  for different values of the particle size  $L$  (in terms of the quantum temperature  $T_L / k^2 = L^2$ ). As it is clearly seen in this picture, the smaller the particle size (hence, the larger the quantization temperature  $T_L$ ), the more finite size related oscillations (minima) should be observed in the temperature dependence of the magnetization  $M_L(T)$ . For example, in our particular case (with  $L = 10\text{nm}$  and  $T_L = 0.15T_c$ ) only "ground state" minimum (corresponding to  $n = 0$ ) is expected to be visible at non-zero temperature  $T_m = 0.05T_c = 15\text{K}$ , in agreement with the observations (see Fig.1). And finally, it should be mentioned that a similar magnetization peak around 50K has been also observed in carbon nanotubes [20] and carbon nanosphere powder [12], where its origin was attributed to adsorbed oxygen and first-order spin reorientation transition, respectively.

In summary, some interesting experimental results related to low- and high-temperature features of the zero-field-cooled magnetization in bulk magnetic graphite have been presented and discussed. The proposed theoretical interpretation for intragranular and intergranular contributions was based, respectively, on superexchange interaction between defects induced localized spins in a single grain and proximity mediated interaction between grains (through the barriers created by thin layers of non-magnetic graphite).

This work has been financially supported by the Brazilian agencies CNPq, CAPES and FAPESP.

---

[1] T. M. Akarova and F. Palacio, Carbon-based magnetism (Elsevier, Amsterdam, 2006).

[2] H. Kronmüller and S. Parkin, Handbook of Magnetism and Advanced Magnetic Materials (John Wiley, Chichester, 2007).

[3] M. J. Katsnelson, Mater. Today 10, 20 (2007).

[4] H. Xia, W. Li, Y. Song, X. Yang, X. Liu and M. Zhao,

Adv. Mater. 20, 4679 (2008).

[5] J. Barzola-Quiza, P. Esquinazi, M. Rothemel, D. Spemann, and T. Butz, J. Nuclear Mater. 389, 336 (2009).

[6] M. Maniyama, K. Kusakabe, S. Tsuneyuki, K. Akagi, Y. Yoshimoto, and J. Yamachi, J. Phys. Chem. Solids 65, 119 (2004).

[7] A. W. Momburu, H. Pardo, R. Faccio, O. F. de Lima, A. J. C. Lanfredi, C. A. Cardoso, E. R. Leite, G. Zanelatto, and F. M. Araujo-Moreira, Phys. Rev. B 71, 100404(R) (2005).

[8] A. V. Rode, E. G. Gamaly, A. G. Christy, J. G. Fitzgerald, S. T. Hyde, R. G. Elliman, B. Luther-Davies, A. I. Veinger, J. Androulakis, and J. Giapintzakis, Phys. Rev. B 70, 054407 (2004).

[9] T. L. Makarova, K. H. Han, P. Esquinazi, R. R. da Silva, Y. Kopelevich, I. B. Zakharaeva, and B. Sundqvist, Carbon 41, 1575 (2003).

[10] Y. Kopelevich, R. R. da Silva, J. H. S. Torres, A. Penicaud, and T. K. Votani, Phys. Rev. B 68, 092408 (2003).

[11] S. Bandow, F. Kokai, K. Takahashi, M. Yudasaka, and S. Iijima, Appl. Phys. A: Mater. Sci. Process. 73, 281 (2001).

[12] R. Caudillo, X. Gao, R. Escudero, M. Jose-Yacamán, and J. B. Goodenough, Phys. Rev. B 74, 214418 (2006).

[13] F. M. Araujo-Moreira, H. Pardo, and A. W. Momburu, Patent WO/2005/123580, World Intellectual Property Organization, Singapore, 2005.

[14] H. Pardo, R. Faccio and A. W. Momburu, F. M. Araujo-Moreira, and O. F. de Lima, Carbon 44, 565 (2006).

[15] S. Sergeenkov, H. Bougrine, M. Ausbos, and R. Clots, JETP Lett. 69, 858 (1999).

[16] S. Sergeenkov, J. Mucha, M. Pekala, V. Drozd, and M. Ausbos, J. Appl. Phys. 102, 083916 (2007).

[17] C. Kittel, Introduction to Solid State Physics (John Wiley, New York, 1996).

[18] R. Faccio, H. Pardo, P. A. Denis, R. Yoshikawa-Oeiras, F. M. Araujo-Moreira, M. Verissimo-Alves, and A. W. Momburu, Phys. Rev. B 77, 035416 (2008).

[19] Y. Shibayama, H. Sato, T. Enoki, and M. Endo, Phys. Rev. Lett. 84, 1744 (2000).

[20] S. Bandow, T. Yamaguchi, and S. Iijima, Chem. Phys. Lett. 401, 380 (2005).